CELL CYCLE
2023, VOL. 22, NOS. 21–22, 2361–2380
https://doi.org/10.1080/15384101.2023.2287367

Taylor & Francis
Taylor & Francis Group

RESEARCH PAPER

Methylation of lncSHGL promotes adipocyte differentiation by regulating miR-149/Mospd3 axis

Xianwei Huang[a,b], Xiong Liu[a,b], and Jiyan Lin[a,b]

[a]Emergency Department, The First Affiliated Hospital of Xiamen University, Xiamen, China; [b]Emergency Department, Xiamen Key Laboratory for Clinical Efficacy and Evidence-Based Research of Traditional Chinese Medicine, Xiamen, China

ABSTRACT

Obesity poses significant health risks and can negatively impact an individual's quality of life. The human obesity phenotype results from the differentiation of pre-adipocytes into adipocytes, which leads to hypertrophy and hyperplasia in adipose tissue. The molecular mechanisms by which long non-coding RNAs (lncRNAs) modulate adipocyte differentiation, a process implicated in obesity development, remain poorly characterized. A lncRNA which suppressed the hepatic gluconeogenesis and lipogenesis (lncSHGL) was newly identified. Our research aims to elucidate the functional role and mechanistic underpinnings of suppressor of lncSHGL in adipocyte differentiation. We observed that lncSHGL expression progressively diminished during 3T3-L1 differentiation and was downregulated in the liver and perirenal adipose tissue of ob/ob mice. lncSHGL acts as a molecular sponge for miR-149, with Mospd3 identified as a target of miR-149.Overexpression of lncSHGL and inhibition of miR-149 led to suppressed 3T3-L1 proliferation, decreased lipid droplet accumulation, and attenuated promoter activity of PPARγ2 and C/EBPα. These changes consequently resulted in reduced expression of Cyclin D1, LPL, PPARγ2, AP2, and C/EBPα, as well as inhibited the PI3K/AKT/mTOR signaling pathway. In contrast, lncSHGL suppression yielded opposing outcomes. Moreover, the effects of lncSHGL overexpression and miR-149 inhibition on reduced expression of Cyclin D1, LPL, PPARγ2, AP2, and C/EBPα were reversible upon miR-149 overexpression and Mospd3 suppression. These findings were further validated *in vivo*. We also discovered a significant increase in methylation levels during 3T3-L1 differentiation, with lncSHGL highly expressed in the presence of a methylation inhibitor. In conclusion. lncSHGL methylation facilitates adipocyte differentiation by modulating the miR-149/Mospd3 axis. Targeting lncSHGL expression may represent a promising therapeutic strategy for obesity-associated adipogenesis, particularly in the context of fatty liver disease.

ARTICLE HISTORY
Received 9 February 2023
Revised 17 April 2023
Accepted 10 November 2023

KEYWORDS
Adipocyte differentiation; lncSHGL; miR-149/Mospd3

Introduction

Obesity is caused by multiple complex factors. It is characterized by excessive body fat and often accompanied by comorbidities, including atherosclerosis, hyperlipidemia, fatty liver disease, and diabetes [1]. The human obesity phenotype is caused by the transformation of pre-adipocytes into adipocytes due to hypertrophy and hyperplasia of the adipose tissue [2]. Abnormal metabolism and fat cell function are core mechanisms leading to obesity [3]. The molecular regulation of adipocyte differentiation and its relationship with the pathogenesis of obesity is a hot spot in medical research in recent years. Effective inhibition of adipocyte differentiation has become an important way to prevent and treat obesity and the range of cardiovascular and metabolic diseases it causes.

The proliferation and differentiation of preadipocytes play a crucial role in maintaining the number and renewal of adipocytes, and they are closely related to the morphology and function of adipocytes [4]. With the development of next-generation sequencing, bovine KLF6 was identified as a regulator of adipogenesis [5,6]. Long non-coding RNA (lncRNAs) have a transcription length of more than 200 nucleotides with no protein-coding function [7,8]. Increasing evidence has demonstrated that lncRNAs play a vital role in many biological processes, including epigenetic

CONTACT Jiyan Lin hxw20126@xmu.edu.cn Emergency Department, The First Affiliated Hospital of Xiamen University, No. 55 Zhenhai Road, Siming District, Xiamen, Fujian Province 361003, China

regulation, cell cycle regulation, cell differentiation regulation, and adipocyte differentiation [7]. Zhang et al. demonstrated LncPRRX1 promoted bovine myoblast proliferation by regulating the miR-137/CDC42 axis [9]. Ma et al. illustrated the critical role of lncRNA BIANCR in intramuscular adipogenesis [10]. Wang et al. observed increased expression of Lnc-OAD during 3T3-L1 differentiation, and that knockdown of lnc-OAD suppressed adipocyte differentiation of 3T3-L1 cells by reducing the expression of PPAR-γ and C/EBPα, which are the adipocyte master transcription factors [11]. Chen et al. found that the expression of lnc-U90926 is reduced during the differentiation of 3T3-L1 cells and in the visceral adipose tissue of obese mice [12]. Overexpression of lnc-U90926 led to a delay 3T3-L1 adipocyte differentiation by decreasing the expression of PPARγ2, FABP4, and AdipoQ [13]. These results suggest that lncRNAs regulate the expression of master genes in adipocytes to maintain adipocyte differentiation. Therefore, a better understanding of the role of lncRNAs in adipogenesis is essential. Moreover, the regulatory mechanism of lncRNAs which contribute to adipocyte differentiation is largely unknown.

In a previous study, lncSHGL was initially identified as AK143693 with a length of 1928 base pairs and is highly expressed in the mouse liver with unknown function [14,15]. Further research indicates that overexpression of lncSHGL suppresses hepatic gluconeogenesis and lipogenesis by recruiting hnRNPA1 [16]. However, the regulatory mechanisms of lncSHGL in adipocyte differentiation remain unclear. Methylation is a process in which a methyl group (CH3) is added to the DNA molecule or its associated proteins. Increasing evidence illustrated the significant role of demethylase and methyltransferase in biological process. For example, Yang et al. illustrated a negative feedback regulatory loop between DNA demethylase gene TET1 and m^6A methyltransferase gene METTL3 in myoblast differentiation [17]. MEFTTL3 was reported to promote MEF2C protein expression through posttranscriptional modification in an m6A-YTHDF1-dependent manner [18]. Moreover, study observed that METTL3-mediated lncRNA EN_42575 exerted a regulatory effect on IPEC-J2 cells exposed to CPB2 toxins [19]. Wang et al. reported induction of m6A methylation in adipocyte exosomal LncRNAs mediating myeloma drug resistance [20]. Thus, there are urgent needs in understanding the methylation of lncSHGL during adipocyte differentiation. One system that has been thoroughly investigated for adipocyte differentiation is the *in vitro*-induced adipocyte differentiation of 3T3-L1 cells. This system recapitulates the major process in adipogenesis *in vivo* [21]. Our study focused on the role of lncSHGL in adipocyte differentiation *in vitro* and in ob/ob mice, with the aim to provide new targets for lncRNAs in the treatment of obesity.

Materials and methods

Adipocyte differentiation

Preadipocytes 3T3-L1 cells were obtained from ImmoCell Biotechnology Co., Ltd. (Xiamen, China) and cultured in DMEM supplemented with 10% newborn calf serum (Genview, GD3103-500 ML). Adipocyte differentiation was induced as described previously [7]. Cells were treated with 1 μmol/L dexamethasone (Sigma), 1 μg/mL insulin (Signma), and 0.5 mmol/L 3-isobutyl-1-methylxanthine (IBMX, Sigma) when the cells passaged at 70–80% confluence on day 0. The medium was then changed to DMEM supplemented with 10% fetal bovine serum (FBS, Gibco) and 1 μg/mL insulin on day 2. During the entire 12-day differentiation process of 3T3-L1 preadipocytes, the culture medium was replaced with DMEM supplemented with 10% fetal bovine serum (FBS, Gibco), which was refreshed every two days. The process of 3T3-L1 adipocyte differentiation was observed using Oil Red O staining. Cells were cultured in an incubator (Thermofisher) under 37°C and supplemented with 5% CO_2.

Oil red O staining

For oil red O staining, we referred to the previous methods [22], and made some minor adjustments. Preadipocytes 3T3-L1 cells were collected at 0, 2, 4, 6, 8, and 12 d after differentiation. The cells were fixed in 70% ethanol for 5 min. After three washes with PBS, the cells were stained with Oil Red O solution (Solarbio, G1262) for 1 h at 25°C.

Images were visualized by light microscopy and photographed after excess stain was removed using 70% isopropyl alcohol.

Cell transfection

After differentiation for 8 days, preadipocytes 3T3-L1 cells were used for further experiments. Transfection was performed in 3T3-L1 cells, which were cultured in DMEM supplemented with 10% fetal bovine serum reached 60–90% confluence. Lipofectamine 2000 (Cat. No. 52887) was used to transfect the cells with lncSHGL shRNA, miR-149, or Mospd3. After 48 hours of transfection, the cells were collected and used for further study, such as CCK8 assay and western blot. The forward and reverse sequence of lncSHGL shRNA1 as following: 5"-AUUCUCUGGACCCUUGCUACUACUG-3' and 5'-CAGUAGUAGCAAGGGUC- CAGAGAAU-3'. The forward and reverse sequence of lncSHGL shRNA2 as following: 5'-GCGCUUACUGGAAGCUCUAAGUGGA-3' and 5'-UCCACUUAGAGCUUCCAGUAAGCGC-3".

Cell-counting kit 8 (CCK-8) assay

CCK-8 assay was used to assess the proliferation of 3T3-L1 cells. Preadipocytes 3T3-L1 cells were collected and 4,000 cells/well were seeded in a 96-well plate. After culturing for different times, the cells were refreshed with 90 μL and 10 μL Cell Counting Kit-8 (Dojindo) for each well in a 96-well plate. The cells were incubated for 2 h at 37°C. Absorbance was measured at 450 nm using a microplate reader (OLYMPUS, CX41).

EdU labeling assay

The EdU labeling kit (RIBOBIO, Cat. No. C10327) was used to further detect the proliferation of 3T3-L1 cells under the different treatments. Briefly, 1×10^5 cells were treated with 10 μM EdU for 1 h at 37°C. The cells were then fixed with 4% formaldehyde and permeabilized with 0.5% Triton X-100 for 10 min. After washing with PBS, the cells were incubated with 400 μL Apollo ® reaction cocktail for 30 min and washed three times with PBS. The DNA was stained with Hoechst 33,342 (5 μg/mL, 500 μL/well) for 30 min. Images were captured using a confocal microscope (Zeiss LSM710). Image J software was used for cell counting analysis [23].

Quantitative real time polymerase chain reaction (qRT-PCR)

TRIzol (Takara, 9109) was utilized to extract the total RNA from the 3T3-L1 cells and tissues. The Bestar qPCR kit (DBI) was used for cDNA synthesis, and the concentration of cDNA was measured using NanoDrop. qRT-PCR was then performed on a Stratagene ReaL time PCR system (Mx3000p, Agilent) with BestarTM qPCR MasterMix (2043, DBI under the following conditions: 95°C for 2 min, 40 cycles of 94°C for 20 s, 58°C for 20 s, and 72°C for 20 s. β-Actin and U6 were used as mRNA and miRNA internal controls, respectively. The relative gene expression was calculated using the 2-ΔΔCq method. The primers used in this study are listed in Table 1.

Table 1. The primers used for qRT-PCR.

ID	Forward Sequence (5′ – 3′)	Reverse Sequence (5′ – 3′)
β-actin	CATTGCTGACAGGATGCAGA	CTGCTGGAAGGTGGACAGTGA
LncSHGL	ACAAATGATGGAGGGCCTGG	GGCAGGTCCCACGAAATACA
LPL	GGGAGTTTGGCTCCAGAGTTT	TGTGTCTTCAGGGGTCCTTAG
PPARγ2	TCGCTGATGCACTGCCTATG	GAGAGGTCCACAGAGCTGATT
FABP4/AP2	AAGGTGAAGAGCATCATAACCCT	TCACGCCTTTCATAACACATTCC
C/EBPα	CAAGAACAGCAACGAGTACCG	GTCACTGGTCAACTCCAGCAC
DNMT1	AAGAATGGTGTTGTCTACCGAC	CATCCAGGTTGCTCCCCTTG
Mospd3	CTGGTCTTTCCCCCGGATCTA	ACAGAACTCGGAAGCGAAGC
Cyclin D1	GCGTACCCTGACACCAATCTC	CTCCTCTTCGCACTTCTGCTC
U6	CTCGCTTCGGCAGCACA	AACGCTTCACGAATTTGCGT
miR-149-3p	CTCAACTGGTGTCGTGGAGT	ACACTCCAGCTGGGGAG
	CGGCAATTCAGTTGAGGCACCGCC	GGAGGGACGGGGGCG

Western blotting

The proteins of cell and tissue samples were lysed with RIPA lysis buffer (Beyotime, Shanghai), and the protein concentrations were measured using the BCA Protein Assay kit (Thermo). Proteins (10 μg/well) were loaded and separated using 10% SDS-PAGE and then transferred onto PVDF membranes (IPVH00010, Millipore). The membrane was blocked with 5% skimmed milk at room temperature for 30 min. Subsequently, the membrane was incubated with primary antibody Mospd3 (1: 1000, 26168–1-AP, proteintech), Cyclin D1 (1: 1000, 26939–1-AP, proteintech), PPARγ2 (1: 1000, ab178868, abcam), C/EBPα (1: 1000, 18311–1-AP, proteintech), LPL (1:6000, 55208–1-AP, proteintech), PI3K (1: 4000, 67071–1-Ig, proteintech), AKT (1: 8000, 10176–2-AP, proteintech), p-PI3K (1: 1000, ab278545, abcam), p-AKT (1: 8000, 66444–1-Ig, proteintech), FABP4/AP2 (1:10000, 12802–1-AP, proteintech), mTOR (1:10000, 66888–1-Ig, proteintech), p-mTOR (1:10000, ab109628, abcam), and GAPDH(1:10000, abcam, ab8245) at 4°C overnight. The membrane was incubated at 25°C with a diluted secondary antibody for 1.5 h. Protein bands were visualized using an enhanced chemiluminescence kit (Millipore, KLS0500) and imaged using MICROTEK (Bio-5000). The relative protein expression was quantified using ImageJ according to the chemiluminescence of the bands.

Immunofluorescence assay

The 3T3-L1 cells were collected and seeded onto coverslips in 24-well plates at 40–60% density. After culturing for 24 h, cells were washed twice with PBS and fixed with 4% paraformaldehyde for 30 min at 25°C. The cells were permeabilized using 0.1% Triton X-100 for 10 min and blocked for 30 min at 25°C after treatment with NH_4Cl solution. The cells were incubated with Mospd3 (1:100, 26168–1-AP, Proteintech) for 2 h at 25°C. The cells were incubated with diluted 488-conjugated secondary antibodies (Life Technologies) for 2 h in the dark at 25°C. The nuclei were stained with 4, 6-diamidino-2-phenylindole (DAPI) for 1 min at 25°C in the dark. The images were observed using a laser scanning confocal microscope (Zeiss, LSM710). Cell counting was performed using ImageJ software.

Luciferase reporter assay

The target sequences of lncSHGL and Mospd3, containing wild-type and mutant binding sites, were cloned into the psiCHECK-2 vector. The promoter sequence of PPARγ2 and C/EBPαcontaining with wild type and mutant binding sites was cloned into the pGL3-Basic vector, respectively. The psiCHECK-2-lncSHGL or Mospd3 with miR-149 mimics were co-transfected with lipofectamine 3000 transfection reagent (Thermo) into 3T3-L1 preadipocytes at a cell density of 60–90%, respectively. For PPARγ2 and C/EBPα, the PPARγ2 and C/EBPα-pGL3-basic vector was transfected into overexpressing or/and suppressing lncSHGL, Mospd3 and miR-149 in 3T3-L1 cells, respectively, 100 ng pRL-TK (a Renilla luciferase plasmid) act as control. A dual Luciferase reporter assay kit (Beyotime, Shanghai, China) was used to detect luciferase activity.

DNA methylation analysis

DNA from 3T3-L1 preadipocytes or cells treated with the methyltransferase inhibitor 5-Aza-dC was extracted using a DNA extraction kit (Biospin, Hangzhou). The EpiTect Fast DNA Bisulfite Kit (Qiagen) was used to extract genomic DNA. Methylation-specific PCR was performed under the conditions: 95°C for 3 min, 95°C for 15 s, 58°C for 15 s, and 72°C for 30 s, followed by 40 cycles at 72°C for 5 min. The products of methylation-specific PCR were separated by agarose gel electrophoresis for 25 min at 120 V and the image was captured using a UV Transmission Analyzer (ZF1-II, JIapenf Biotech, Shanghai). The primers were designed based on the CpG sites on the lncSHGL promoter. The U primer was Forward: 5'-TTTATTTGTATGTAATAGGACGCGT-3,' Reverse:5'-CTAAATTAATAAAAAAAACCCCGTT-3'and the M primer was Forward: 5'-TTTATTTGTATGTAATAGGATGTGT-3,' Reverse: 5'- CCTCTAAATTAATAAAAAAAACCCCAT-3.'

Immunoprecipitation assay

Cells (2.0×10^6 per well) were seeded into a 6-well plate and transfected with miR-149 mimics when the confluence reached 60–90%.

Cells were lysed using radioimmunoprecipitation assay (RIPA) buffer after transfection for 24 h. Before co-precipitation, the Mospd3 or lncSHGL probe antibody was incubated with protein G magnetic beads for 12 h at 4°C. The lysate was co-immunoprecipitated with protein G magnetic beads for 4 h at 25°C. To remove nonspecific binding, 25 µL of blocked protein G Dynabeads (Life Technologies) was added to each sample, incubated for 1 h at 4°C, and then removed with a magnetic field. Finally, the samples were treated with proteinase K and SDS to degrade Argonaute protein, disrupt antibody binding and elute RNA from magnetic beads, and treated with DNase I. The eluted RNA was resuspended in 30 µL of RNase-free water and maintained at −80°C. An IgG antibody (#5415, Cell Signaling Technology) was used as a negative control (NC). qRT-PCR was performed as described for qRT-PCR.

Animal model and analyses

Seven-week-old male C57BL/6 and ob/ob mice were purchased from Model Organisms Co. Ltd. (Shanghai, China). C57BL/6 and ob/ob mice were fed a basal diet (5% fat) and a high-fat diet (HFD) (20% fat) under a 12 h light-dark cycle with free access to water and food for one week [24]. The C57BL/6 mice were randomly divided into four groups: a control group with a basal diet, ob/ob group with a HFD, NC and lncSHGL group, NC, and lncSHGL adenovirus was injected by tail vein for 14 days in ob/ob mice with HFD. These ob/ob mice were fed a HFD until their body weights of were 30% greater than that of the control mice, then these transgenic obese mice and the control mice were analyzed. Triglyceride (TG, MAK266, Sigma) and total cholesterol (TC, CS0005, Sigma) from serum were detected using an ELISA Kit according to the manufacturer's instructions. This animal study was reviewed and approved by the ethics committee of the first Affiliated Hospital of Xiamen University.

H&E staining

For H&E staining, we referred the protocol in published paper [25]. The livers of mice were removed and fixed with 4% paraformaldehyde at 37°C for 24 h. Specimens were then dehydrated, embedded, and cut into 5 µm thickness slices according to the manufacturer's instructions. The slices were stained with Harris (Servicebio, G1004) for 4 min, divided for a few seconds with 1% hydrochloric acid alcohol, rinsed with tap water, returned to blue color with 0.6% ammonia water, and rinsed with running water. The slices were stained with eosin dye (Servicebio, G1005) for 3 min. Subsequently, the slices were dehydrated and sealed with neutral resin. Images were captured using an inverted fluorescence microscope (Nikon Eclipse E100).

Statistical analysis

All data, presented as the mean ± s.e.m., were analyzed and visualized using Graph Pad Prism software (version 8.0). The unpaired student's t-test was performed to calculate the significance between the two groups. Statistical significance was set at $P < 0.05$.

Results

lncSHGL gradually decreased during 3T3-L1 preadipocytes differentiation

To investigate the role of lncSHGL in the differentiation process of 3T3-L1 preadipocyte cells, we employed qRT-PCR to measure lncSHGL expression. We first induced 3T3-L1 cell differentiation and observed that, according to Figure 1a, the intensity of Oil Red O staining demonstrated a significant accumulation of lipid droplets following a 2-day induction period. A high quantity of lipid droplets was evident on days 8 and 12. Concurrently, the expression levels of adipocyte marker genes, such as LPL, PPARγ2, AP2, and C/EBPα, progressively increased during 3T3-L1 preadipocyte differentiation, reaching peak levels after 8 days of induction (Figure 1b-e). This observation confirmed the successful induction of 3T3-L1 cell differentiation. Given that lncSHGL has been previously implicated in the regulation of lipid metabolism [10], we examined its expression during 3T3-L1 cell differentiation. Intriguingly, we discovered that lncSHGL expression steadily

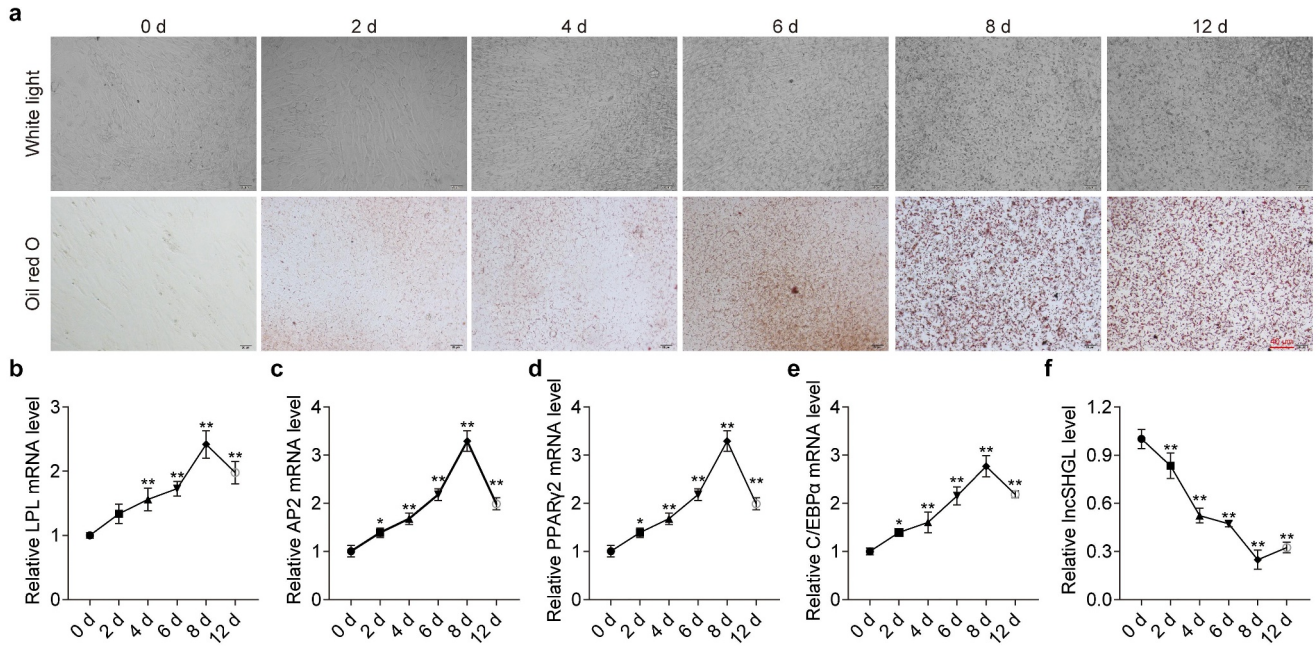

Figure 1. LncSHGL was gradually decrease during 3T3-L1 preadipocytes differentiation. a, Oil red O staining was used to detect lipid droplet at 0, 2, 4, 6, 8 and 12 days during 3T3-L1 preadipocytes differentiation, Bar = 20 μm; b-e, the expression of adipocyte marker genes LPL, PPARγ2, AP2 and C/EBPα was detected by qRT-PCR during 3T3-L1 preadipocytes differentiation, respectively, GAPDH act as control; F, the expression of LncSHGL was detected by qRT-PCR during 3T3-L1 preadipocytes differentiation; data was represented as mean±SD, $^{**}P < 0.01$, vs 0 day.

decreased as 3T3-L1 preadipocyte cells differentiated, reaching its lowest point after 8 days of induction (Figure 1f). This finding suggests that elevated lncSHGL expression may suppress 3T3-L1 differentiation.

Overexpression of lncSHGL impeded adipocyte differentiation and lipid droplet accumulation

To investigate the role of lncSHGL in adipocyte differentiation and lipid droplet accumulation, we performed overexpression and knockdown of lncSHGL in MDI-stimulated 3T3-L1 preadipocytes (treated with 3-isobutyl-1-methylxanthine [IBMX], dexamethasone [Dex], and insulin). Cells transfected with lncSHGL OE or sh-lncSHGL plasmids exhibited successful overexpression or suppression of lncSHGL, respectively (Figure 2a). The CCK-8 assay revealed that lncSHGL overexpression inhibited 3T3-L1 preadipocyte proliferation, while lncSHGL suppression promoted proliferation (Figure 2b). EdU staining corroborated these findings, with the EdU labeling kit showing a significant decrease in EdU-positive cells upon lncSHGL overexpression and an increase following lncSHGL suppression in MDI-stimulated 3T3-L1 preadipocytes, compared to control and vector groups (Figure 2c).

Oil Red O staining demonstrated that lncSHGL overexpression substantially reduced lipid droplet accumulation, while lncSHGL suppression increased accumulation in MDI-stimulated 3T3-L1 preadipocytes (Figure 2d). Triglyceride (TG) content changes were consistent with the observed alterations in lipid droplet accumulation induced by lncSHGL (Figure 2e). Furthermore, both mRNA and protein expression levels of adipocyte marker genes, including Cyclin D1, LPL, PPARγ2, AP2, and C/EBPα, were markedly downregulated upon lncSHGL overexpression and upregulated upon lncSHGL suppression (Figure 2f,g). These findings indicate that lncSHGL overexpression hinders adipocyte differentiation and lipid droplet accumulation.

LncSHGL acts as a sponge of miR-149

To elucidate the molecular impact of lncSHGL on adipocyte differentiation, we employed Starbase v2.0

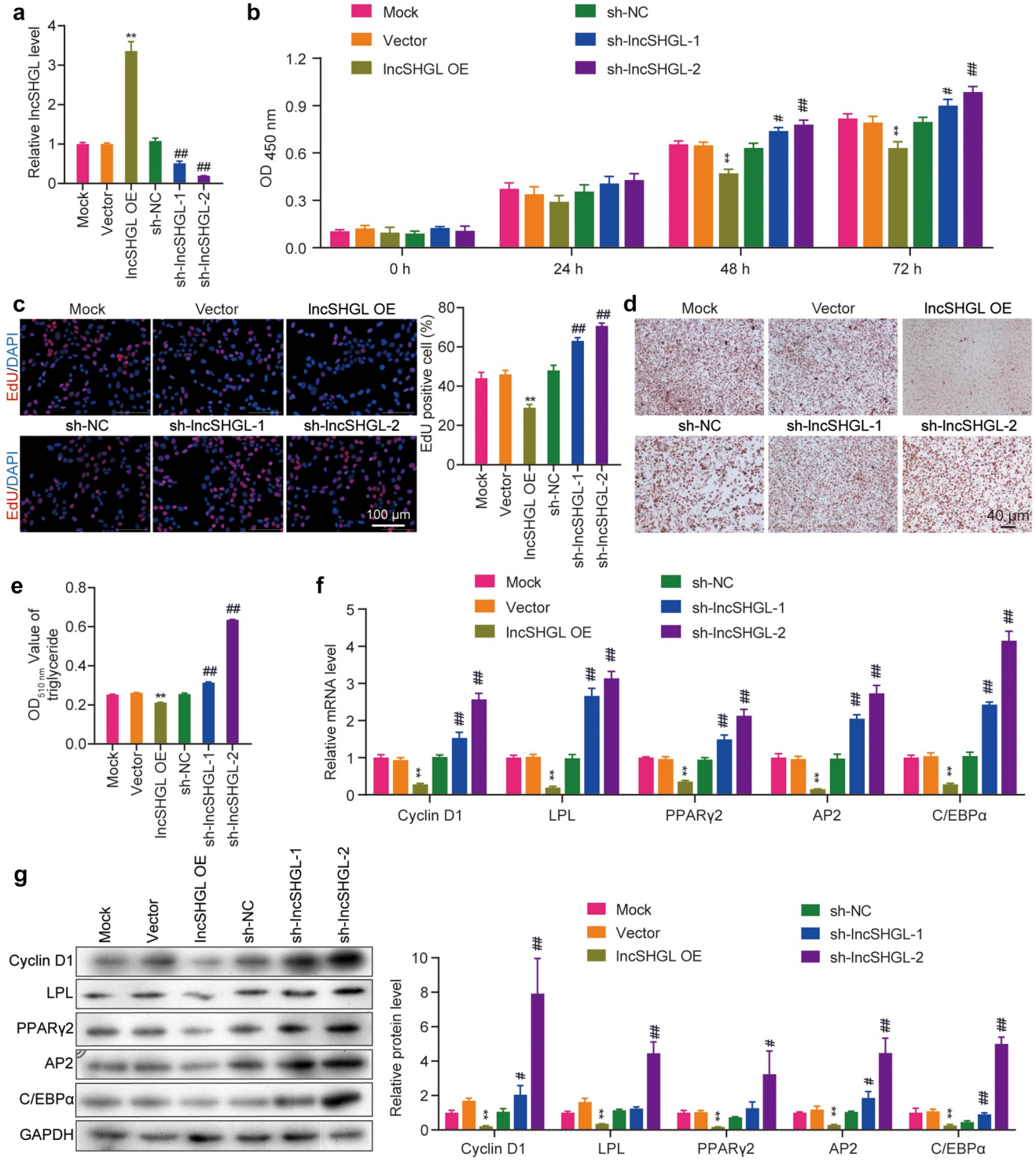

Figure 2. Overexpression LncSHGL impeded adipocyte differentiation and lipid droplet accumulation. a, the expression of LncSHGL was successfully overexpressed or suppressed by transfection with over-LncSHGL or sh-LncSHGL plasmid, respectively; b, CCK-8 analysis was used to detect the proliferation of MDI 3T3-L1 preadipocytes affected by LncSHGL; c, edu analysis was used to detect the proliferation of MDI 3T3-L1 preadipocytes; d, Oil Red O staining was used to detect lipid droplet accumulation affected by LncSHGL increased the lipid droplet accumulation in MDI 3T3-L1 preadipocytes, Bar = 20 μm; e, the contents changes of TG affected by LncSHGL; f and g, qRT-PCR and western blot was used to detect the expression of adipocyte marker genes CyclinD1, LPL, PPARγ2, AP2 and C/EBPα affected by LncSHGL, GAPDH act as control; data was represented as mean±SD, **, $P < 0.01$, lncSHGL (OE) vs NC (OE); ##, $p < 0.01$, sh-lncSHGL vs sh-CTRL.

to predict potential miRNA targets of lncSHGL. Three binding sites on lncSHGL, located at positions 87–108, 445–466, and 1091–1112, were identified as targets for miR-149 (Figure 3a). When cells were co-transfected with wild-type lncSHGL and miR-149 mimic, the relative luciferase activity was significantly reduced compared to the negative control (NC) group. However, no changes in relative luciferase activity were observed in the miR-149 mimic group relative to the NC group when cells were co-transfected with mutant lncSHGL at position 445–466, but not at positions 87–108 or 1091–1112 (Figure 3b). This suggests that lncSHGL can bind with miR-149 at position 445–466.

Additionally, the miR-149 immunoprecipitation experiment revealed that lncSHGL was significantly enriched when immunoprecipitated with miR-149 mimics compared to NC (Figure 3c). miR-149 expression was markedly reduced in cells overexpressing lncSHGL and upregulated in cells with silenced lncSHGL (Figure 3d). These findings indicate that lncSHGL functions as a molecular sponge for miR-149.

miR-149 could partially reverse the function of LncSHGL on adipocyte differentiation and lipid droplet accumulation

To elucidate the role of miR-149 in modulating the effects of lncSHGL on adipocyte differentiation and lipid droplet accumulation, we introduced miR-149 mimics into lncSHGL-overexpressing adipocytes. The

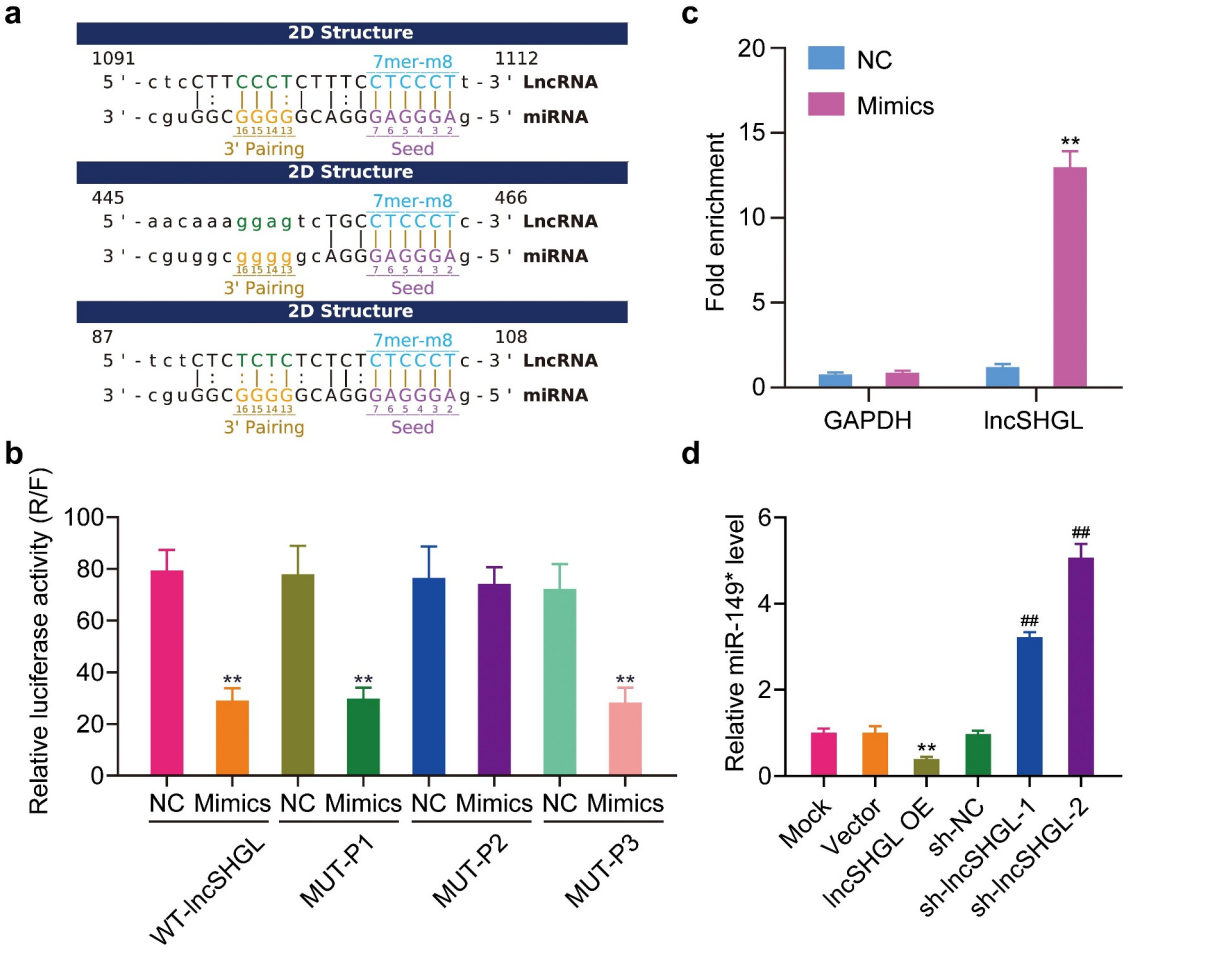

Figure 3. LncSHGL act as a sponge of miR-149. a, xx was used to predict the miRNA targets of LncSHGL and binding sites between LncSHGL and miR-149 located at 87–108, 445–466 and 1091–1112 of LncSHGL, respectively; b, dual luciferase reporter system analysis was used to verify the regulation between LncSHGL and miR-149, **, $P < 0.01$, mimics group Vs NC group; c, miR-149 immunoprecipitation was used to enrich LncSHGL, **, $P < 0.01$, mimics group Vs NC group; d, the expression of miR-149 was detected by qRT-PCR affected by LncSHGL, U6 act as control. Data was represented as mean±SD, **, $P < 0.01$, lncSHGL (OE) group Vs NC (OE) group; ##, $p < 0.01$, sh-lncSHGL group Vs sh-CTRL group.

expression of miR-149 was significantly upregulated in lncSHGL-overexpressing adipocytes treated with miR-149 mimics compared to the negative control (NC) group (Figure 4a). EdU experiments revealed that the number of EdU-positive cells was markedly reduced in lncSHGL-overexpressing adipocytes in the presence of miR-149 mimics relative to the NC group (Figure 4b). Oil Red O staining demonstrated that miR-149 mimics substantially increased lipid droplet accumulation in lncSHGL-overexpressing adipocytes compared to the NC group (Figure 4c). Triglyceride (TG) content also exhibited a significant increase in the presence of miR-149 mimics relative to the NC group (Figure 4d).

Furthermore, qRT-PCR and western blot experiments indicated that the expression of adipocyte marker genes, including Cyclin D1, LPL, PPARγ2, AP2, and C/EBPα, were notably upregulated in the presence of miR-149 compared to the NC group (Figure 4e,f). These findings demonstrate that miR-149 can counteract the effects of lncSHGL on adipocyte differentiation and lipid droplet accumulation.

Mospd3 targeted with miR-149

We utilized TargetScan to investigate the downstream targets of miR-149. As depicted in Figure 5a, the binding site analysis within the 3' untranslated region (UTR) of Mospd3 indicated that miR-149 may regulate Mospd3. The relative luciferase activity was significantly decreased in the miR-149 mimic group compared to the negative control (NC) group when co-transfected with the wild-type Mospd3 binding site. In contrast, no change in relative luciferase activity was observed in the miR-149 mimic group after co-transfection with the mutant Mospd3 binding site (Figure 5a).

Furthermore, the miR-149 immunoprecipitation experiment results showed that Mospd3 was significantly enriched in immunoprecipitates obtained from the miR-149 mimic group, compared to the NC group (Figure 5b). We also found that Mospd3 expression was upregulated in cells overexpressing lncSHGL and downregulated in cells with silenced lncSHGL, compared to the NC group (Figure 5c,d). Additionally,

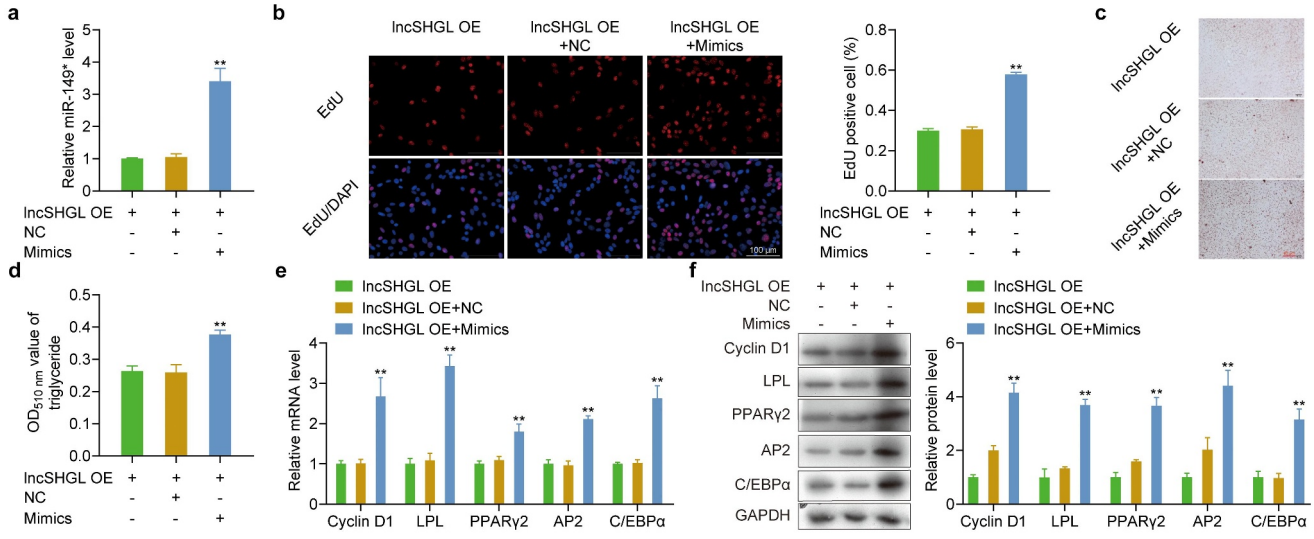

Figure 4. miR-149 could partially reversed the function of LncSHGL on adipocyte differentiation and lipid droplet accumulation. a, the expression of miR-149 was significantly upregulated when treatment with miR-149 mimics; b, edu analysis was used to detect the proliferation of overexpressing LncSHGL adipocyte treatment with miR-149 mimics; c, Oil Red O staining was used to detect lipid droplet accumulation in overexpressing LncSHGL adipocyte treatment with miR-149 mimics, Bar = 20 μm: d, the contents changes of TG in overexpressing LncSHGL adipocyte treatment with miR-149 mimics; e and F, qRT-PCR and western blot was used to detect the expression of adipocyte marker genes CyclinD1, LPL, PPARγ2, AP2 and C/EBPα in overexpressing LncSHGL adipocyte treatment with miR-149 mimics; data was represented as mean±SD, **, $P < 0.01$, lncSHGL (OE) +mimic group vs lncSHGL (OE) group.

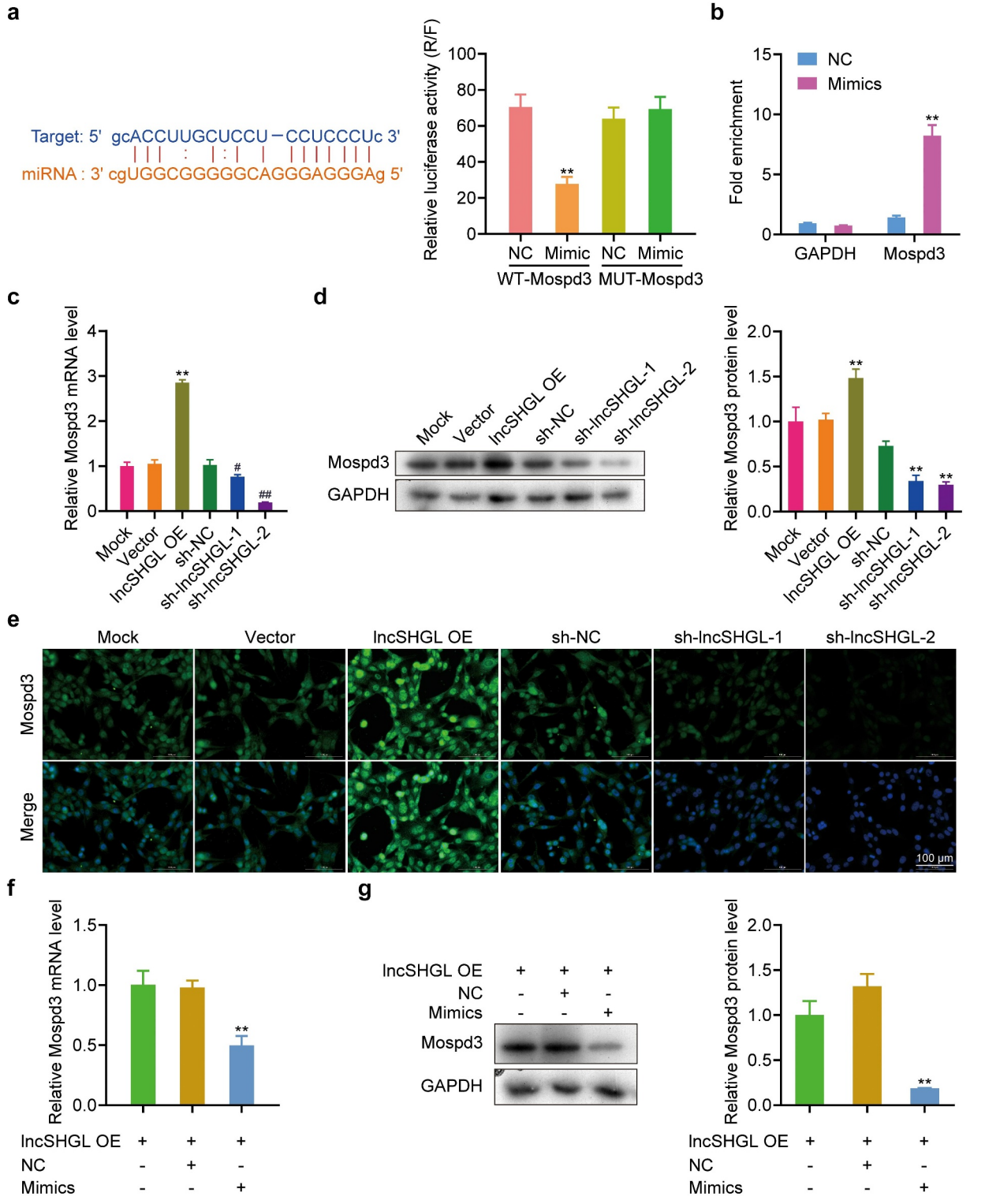

Figure 5. Mospd3 is a target of miR-149. a, bioinformatic analysis predict the binding sites of miR-149 and Mospd3 (left). Dual luciferase reporter system analysis was used to detect the regulation between miR-149 and Mospd3, mimics group vs NC group (right); b, miR-149 immunoprecipitation was used to enrich Mospd3; c and d, qRT-PCR and western blot was used to detect the expression of Mospd3 affected by LncSHGL; e, if was used to detect the expression of Mospd3 affected by LncSHGL, **, $P < 0.01$, lncSHGL (OE) group vs NC (OE) group; ##, $p < 0.01$, sh-lncSHGL group vs sh-CTRL group; f and g, the effect of miR-149 mimics on the expression of Mospd3 affected by LncSHGL, data was represented as mean±SD, **, $P < 0.01$, lncSHGL (OE) +mimic group vs lncSHGL (OE) + NC group.

immunofluorescence experiments demonstrated that Mospd3 fluorescence intensity was significantly increased in cells overexpressing lncSHGL and decreased in cells with silenced lncSHGL compared to the NC group transfected with an empty vector (Figure 5e). The increased Mospd3 mRNA and protein expression induced by lncSHGL overexpression was markedly diminished in the presence of miR-149 mimics (Figure 5f,g), suggesting that Mospd3 is a target of miR-149.

Mospd3 knockdown reversed the function of miR-149 inhibitor on adipocyte differentiation and lipid droplet accumulation

To investigate the role of Mospd3 in adipocyte differentiation and lipid droplet accumulation influenced by miR-149, adipocytes were transfected with Mospd3 siRNA. The expression of Mospd3 was significantly downregulated in Mospd3-silenced adipocytes treated with the miR-149 inhibitor compared to the negative control (NC) group (Figure 6a,b). EdU staining revealed that the number of EdU-positive cells was substantially increased in Mospd3-silenced cells in the presence of the miR-149 inhibitor compared to the NC group (Figure 6c).

Oil Red O staining and TG content analysis indicated that Mospd3 silencing notably promoted lipid droplet accumulation and elevated TG content in the presence of the miR-149 inhibitor compared to the NC group (Figure 6d,e). Additionally, the expression of adipocyte marker genes, including Cyclin D1, LPL, PPARγ2, AP2, and C/EBPα, were markedly upregulated following Mospd3 knockdown

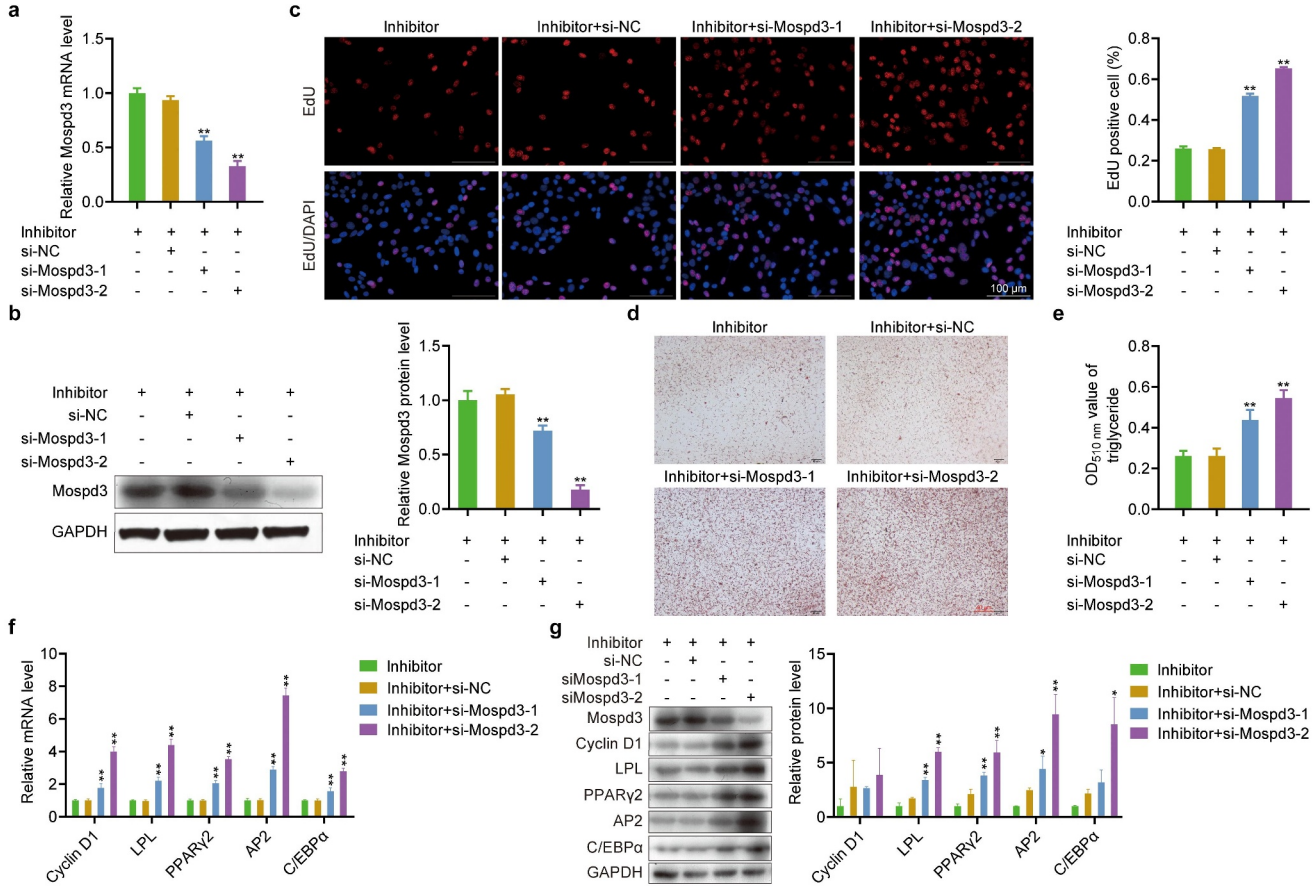

Figure 6. Mospd3 knockdown reversed the function of miR-149 inhibitor on adipocyte differentiation and lipid droplet accumulation. a and b, the expression of Mospd3 was detected by qRT-PCR and western blot treatment with miR-149 inhibitor and SiRNA of Mospd3; c, edu analysis was used to detect the EdU-positive cells treatment with miR-149 inhibitor and SiRNA of Mospd3; d and e, Oil Red O staining and TG contents was used to detect lipid droplet accumulation and TG contents treatment with miR-149 inhibitor and SiRNA of Mospd3, respectively; f and g, qRT-PCR and western blot analysis was used to the expression of adipocyte marker genes CyclinD1, LPL, PPARγ2, AP2 and C/EBPα treatment with miR-149 inhibitor and SiRNA of Mospd3, respectively, GAPDH act as control; data was represented as mean±SD, si Mospd3 group vs NC group.

compared to the NC group (Figure 6f,g). These findings demonstrate that Mospd3 knockdown reverses the effects of the miR-149 inhibitor on adipocyte differentiation and lipid droplet accumulation.

lncSHGL regulated PPARγ2 and C/EBPα expression by regulating the promotor of PPARγ2 and C/EBPα via miR-149/Mospd3 axis

To elucidate the mechanism by which lncSHGL regulates PPARγ2 and C/EBPα expression, we assessed the modulation of PPARγ2 and C/EBPα by lncSHGL through luciferase activity. Overexpression of lncSHGL diminished the relative luciferase activity, while suppression of lncSHGL enhanced the relative luciferase activity compared to the control group, which was transfected with pGL6-PPARγ2 or C/EBPα promoter (Figure 7a,b). Further analysis demonstrated that the relative luciferase activity was significantly increased when treated with miR-149 mimics compared to the NC group (Figure 7c,d). Additionally, we found that the relative luciferase activity was markedly upregulated by treatment with Mospd3 siRNA in miR-149 inhibitor adipocytes compared to the NC group (Figure 7e,f). These results indicate that lncSHGL regulates PPARγ2 and C/EBPα expression by modulating the promoters of PPARγ2 and C/EBPα via the miR-149/Mospd3 axis.

PI3K/AKT signaling pathway is affected by the lncShgl/miR-149/mospd3 axis

To investigate the downstream signaling pathways influenced by lncSHGL, differentially expressed genes (DEGs) between low and high expression groups of lncSHGL were obtained using bioinformatics analysis. GO and KEGG enrichment analyses

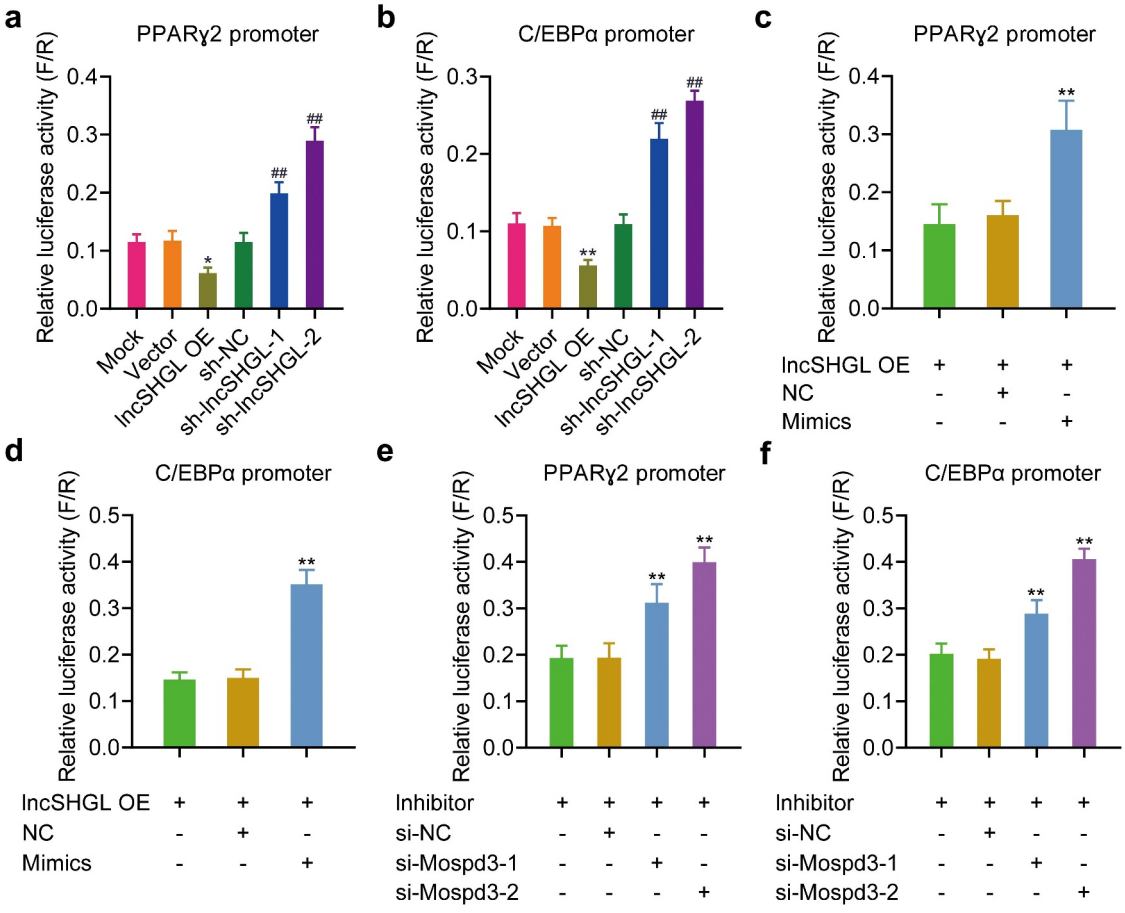

Figure 7. LncSHGL regulated PPAR\γ2 and C/EBPα expression by regulating promotor of PPARγ2 and C/EBPα via miR-149/Mospd3 axis. a and b, dual luciferase reporter system was used to detect the regulation of LncSHGL to PPARγ2 and C/EBPα, **, $P < 0.01$, lncSHGL (OE) group vs NC (OE) group; ##, $p < 0.01$, sh-lncSHGL group vs sh-CTRL group; c and d, the relative luciferase activity was affected by miR-149 mimics, **, $P < 0.01$, lncSHGL (OE) +mimic group vs lncSHGL (OE) + NC group; e and f, the relative luciferase activity was affected by Mospd3 in miR-149 inhibitor adipocyte, data was represented as mean±SD, si Mospd3 group vs NC group.

were performed based on DEGs. The top 10 enriched pathways with the lowest *P* values in the GO biological process, cellular component, and molecular function are shown in Figure 8a. KEGG enrichment analysis indicated that the PI3K-AKT pathway was the most significantly enriched among high and low lncSHGL expression groups (Figure 8b).

In accordance with the bioinformatic analysis results, the protein expression levels of PI3K/AKT signaling pathway-related genes were detected using western blotting. As shown in Figure 8c, the protein expression levels of phosphorylated PI3K, AKT, and mTOR were significantly reduced in cells overexpressing lncSHGL and upregulated in cells with silenced lncSHGL. Further analysis demonstrated that the reduced expression of phosphorylated PI3K, AKT, and mTOR by lncSHGL overexpression was partially reversed after cells were treated with miR-149 mimics (Figure 8d). Additionally, we found that suppression of Mospd3 increased the expression of phosphorylated PI3K, AKT, and mTOR in 3T3-L1 adipocytes in the presence of the miR-

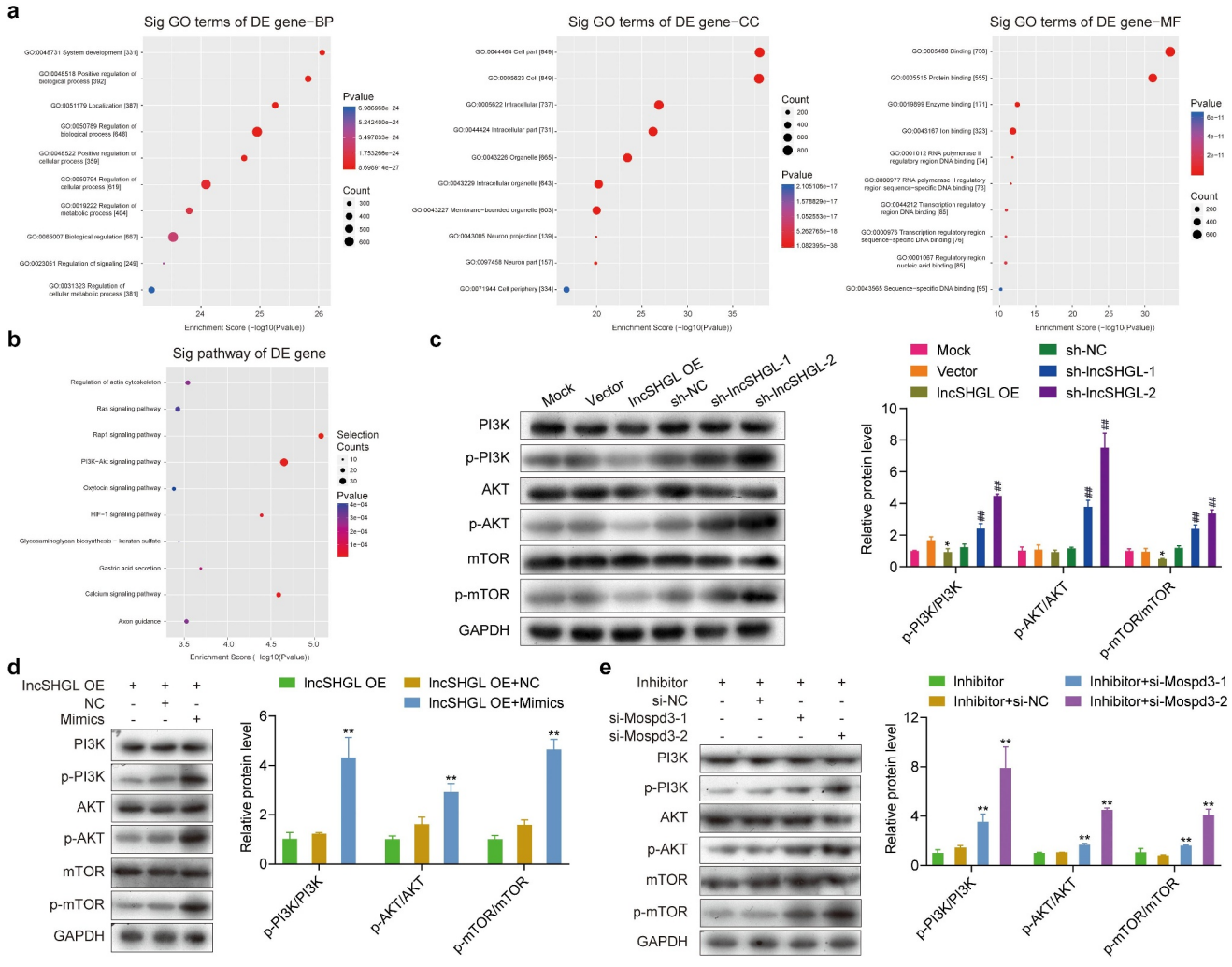

Figure 8. PI3K/AKT signaling pathway was affected by LncSHGL/miR-149/Mospd3 axis. a, go enrichment analysis to the targets of LncSHGL; b, KEGG analysis to the targets of LncSHGL; c, PI3K-AKT signaling pathway related proteins detected by western blot affected by LncSHGL, **, $P < 0.01$, lncSHGL (OE) group vs NC (OE) group; ##, $p < 0.01$, sh-lncSHGL group vs sh-CTRL group; d, PI3K-AKT signaling pathway related proteins detected by western blot affected by miR-149 mimics, **, $P < 0.01$, lncSHGL (OE) +mimic group vs lncSHGL (OE) + NC group; E, PI3K-AKT signaling pathway related proteins detected by western blot affected by Mospd3 in miR-149 inhibitor adipocyte, data was represented as mean±SD, si Mospd3 group vs NC group.

149 inhibitor (Figure 8e). These results suggest that lncSHGL regulates the PI3K/AKT signaling pathway via the miR-149/Mospd3 axis.

DNA methylation was increased in 3T3-L1 cell during differentiation

As DNA methylation plays a crucial role in adipose development [12], we measured DNA methylation levels in MDI-stimulated cells. As shown in Figure 9a, the DNA methylation level was dramatically elevated in the MDI group compared to that in the control group. Further analysis indicated that the expression of DNA methyltransferase 1 (DNMT1), which promotes DNA methylation [13], gradually increased during 3T3-L1 differentiation, and the expression of DNMT1 reached its highest level after 8 days of stimulation (Figure 9b).

To further explore the DNA methylation level during 3T3-L1 cell differentiation, 5-Aza-2'-deoxycytidine (5-Aza-dC), an inhibitor of DNMT1 activity that induces DNA hypomethylation, was used to treat 3T3-L1 cells. The results showed that the DNA methylation level was significantly reduced when cells were treated with 5-Aza-dC (Figure 9c). Further analysis illustrated that the expression levels of DNMT1, LPL, PPARγ2, AP2, and C/EBPα were significantly downregulated, while the expression level of lncSHGL was dramatically upregulated after treating cells with 5-Aza-dC (Figure 9d). This

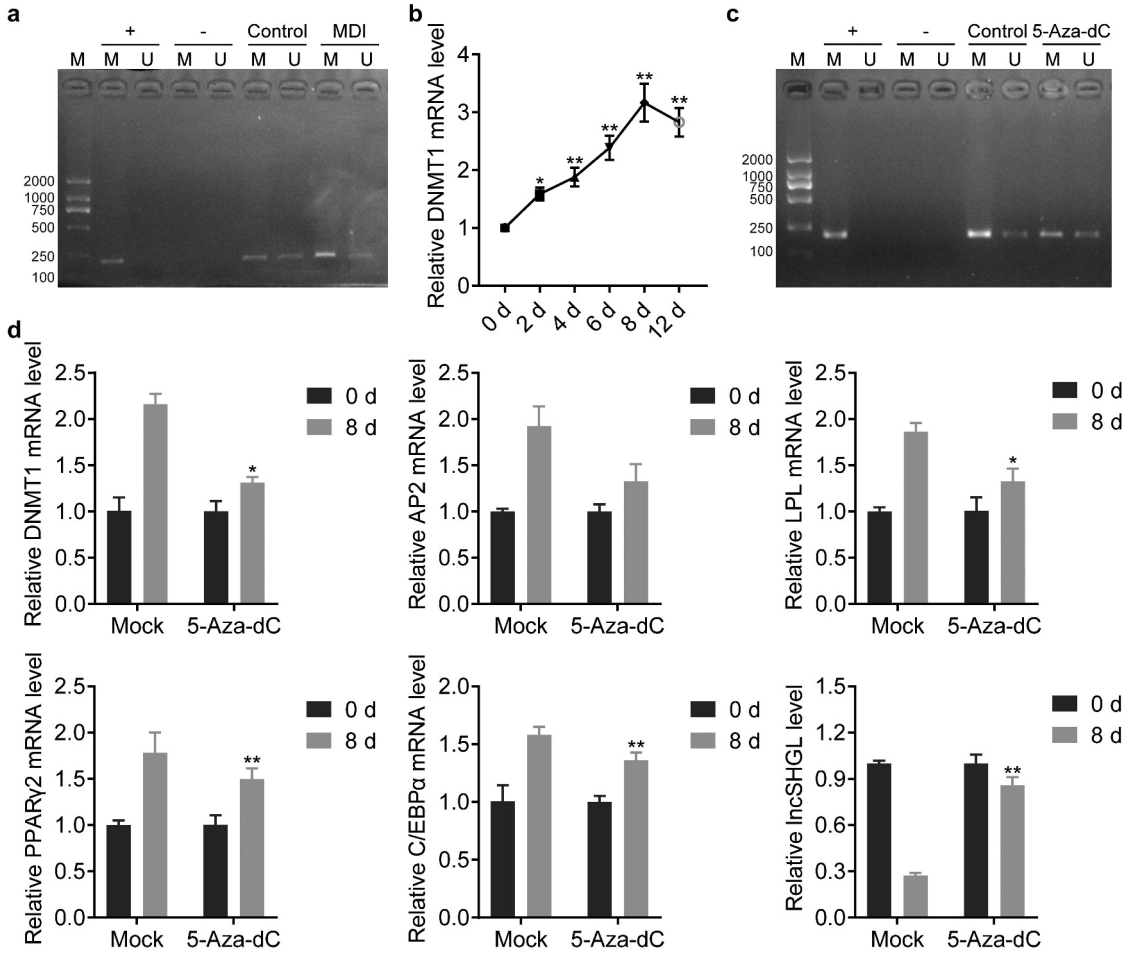

Figure 9. DNA methylation was increased in 3T3-L1 cell during differentiation. a, MSP was used to detect DNA methylation in the 3T3-L1 cell differentiation; b, the expression of DNMT1 qRT-PCR at 0, 2, 4, 6, 8 and 12 days during 3T3-L1 differentiation; c, DNA methylation level was detected by MSP treatment with 5-Aza-dC; d, the expression of DNMT1, LPL, PPARγ2, AP2, C/EBPα and lncSHGL was detected by qRT-PCR in adipocyte treatment with 5-Aza-dC; data was represented as mean±SD, **, $P < 0.01$, 5-Aza-dC group vs control group.

result indicates that the DNA methylation level increased during differentiation. Inhibition of DNA methylation increased the expression of lncSHGL and reduced the expression of adipocyte marker genes.

Lipid droplet accumulation and PI3K/AKT/mTOR signaling pathway were affected by overexpression of LncSHGL in ob/ob mice

To further determine the function of lncSHGL in adipose tissue development, ob/ob mice overexpressing lncSHGL were established. LncSHGL expression was significantly downregulated in the liver and perirenal fat, but not in the subcutaneous fat of ob/ob mice, compared with control mice (Figure 10a). After overexpressing lncSHGL in ob/ob mice, an upregulation of lncSHGL was observed in the liver, but not in the subcutaneous fat or perirenal fat (Figure 10a). Therefore, we focused on the function of lncSHGL in the liver for further analysis.

H&E staining indicated that inflammatory infiltration and injury were dramatically aggravated in ob/ob mice but alleviated after lncSHGL overexpression in ob/ob mice (Figure 10b). Oil Red O staining showed lipid droplet accumulation in ob/ob mice, while overexpression of lncSHGL significantly reduced lipid droplet accumulation in the liver (Figure 10c). Consistent with these results, the contents of total cholesterol and total TG were significantly

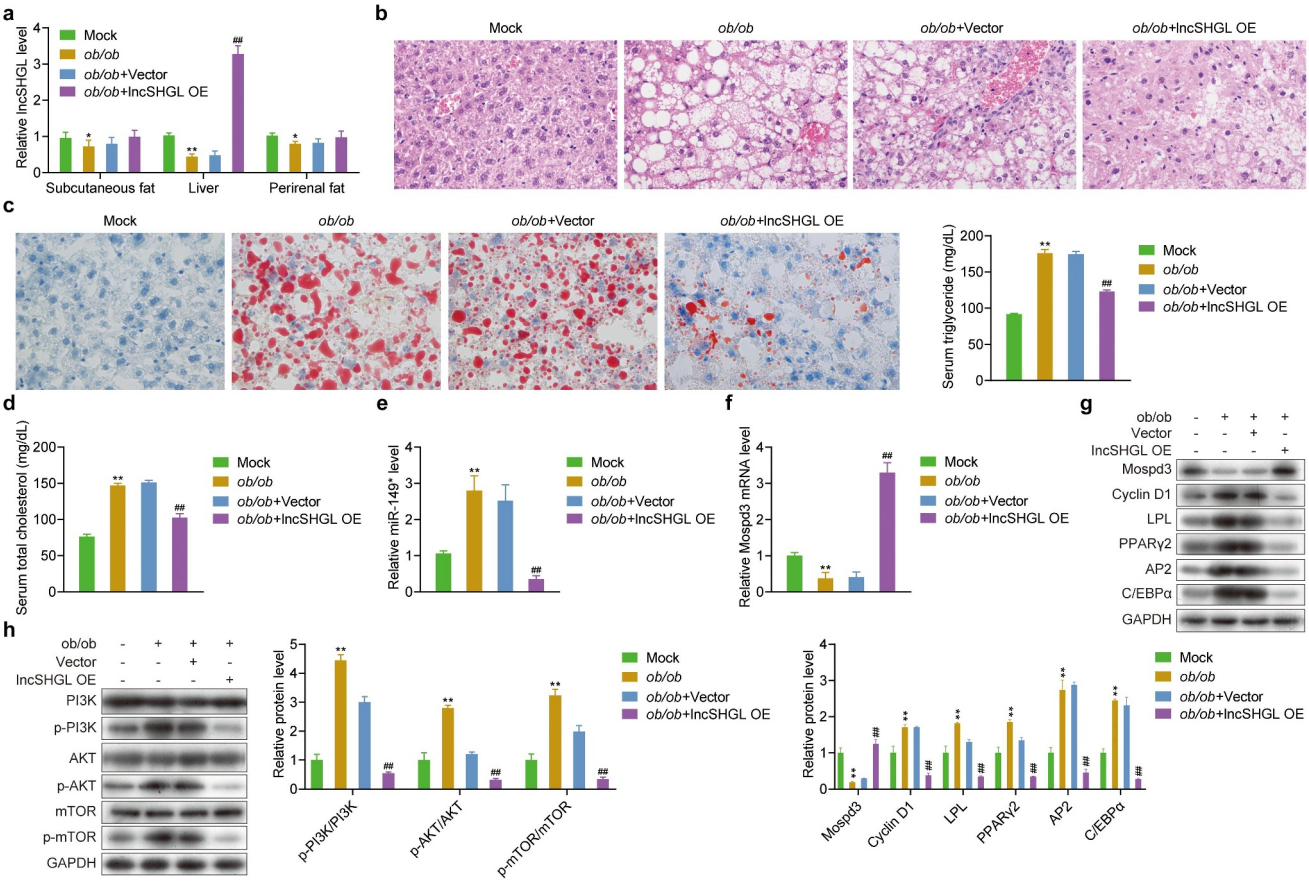

Figure 10. Lipid droplet accumulation and PI3K/AKT/mTOR signaling pathway was affected by overexpression of LncSHGL in ob/ob mice. a, the expression of LncSHGL in subcutaneous, liver and perirenal fat of ob/ob mice after overexpressing LncSHGL; b, H&E staining analysis was used to detect the inflammatory infiltration and injury in ob/ob mice while by overexpressing LncSHGL; c, Oil Red O staining was used to detect lipid droplet accumulation in ob/ob mice with LncSHGL overexpression; d, TC and total TG in liver was detect in ob/ob mice by overexpressing LncSHGL; e and f, the expression of miR-149 and Mospd3 was detected by qRT-PCR in the ob/ob mice by overexpressing LncSHGL; g, the expression of Cyclin D1, LPL, PPARγ2, AP2, C/EBPα was detected by western blot in ob/ob mice by overexpressing LncSHGL; h, the expression of PI3K, AKT and mTOR was detected by western blot affected by LncSHGL in ob/ob mice. Data was represented as mean±SD, **, $P < 0.01$, ob/ob group vs control group; ob/ob +lncSHGL (OE) group vs ob/ob +lncSHGL (NC) group.

increased in ob/ob mice but reduced by overexpression of lncSHGL (Figure 10d).

Furthermore, miR-149 was significantly upregulated in ob/ob mice when compared with control mice, whereas downregulated miR-149 was observed in the overexpressed lncSHGL in ob/ob mice (Figure 10e). However, the changes in Mospd3 expression showed opposite results when compared to miR-149 expression (Figure 10f). Moreover, the expression of Cyclin D1, LPL, PPARγ2, AP2, and C/EBPα were significantly increased in ob/ob mice but decreased in ob/ob mice overexpressing lncSHGL (Figure 10g). In addition, the accumulation of phosphorylated PI3K, AKT, and mTOR proteins was significantly upregulated in ob/ob mice and downregulated in ob/ob mice overexpressing lncSHGL (Figure 10h). The in vivo results were consistent with the in vitro results.

The above data illustrated that lncSHGL overexpression inhibited lipid droplet accumulation in the liver of ob/ob mice via the miR-149/Mospd3 axis. As shown in Figure 11, methylation of lncSHGL promotes adipocyte differentiation by regulating the miR-149/Mospd3 axis. The expression of lncSHG was downregulated by DNA methylation, and Mospd3 was downregulated by sponging miR-149. Finally, the lncSHGL-mediated miR-149/Mospd3 axis would increase the expression of PPARγ2 and C/EBPα and activate the PI3K/AKT signaling pathway, promoting adipocyte differentiation.

Discussion

Obesity has become a serious public health issue worldwide [26]. Obesity is a metabolic abnormality characterized by excessive fat accumulation due to energy imbalance in the body, normally manifesting as an abnormal increase in the number and volume of adipocytes [27]. Therefore, a deep understanding of the mechanisms of adipocyte differentiation is of great significance for the prevention and treatment of obesity. lncRNAs widely participate in various important physiological processes in organisms and regulate the expression of target genes at the transcriptional and post-transcriptional epigenetic levels. Increasing numbers of lncRNAs have been identified in the adipocyte differentiation, such as Plnc1, PVT1, and slincRAD [28–30]. In a previous study, Wang et al. demonstrated that the expression of mouse lncSHGL and its homologous human lncRNA B4GALT1-AS1 was significantly reduced in the

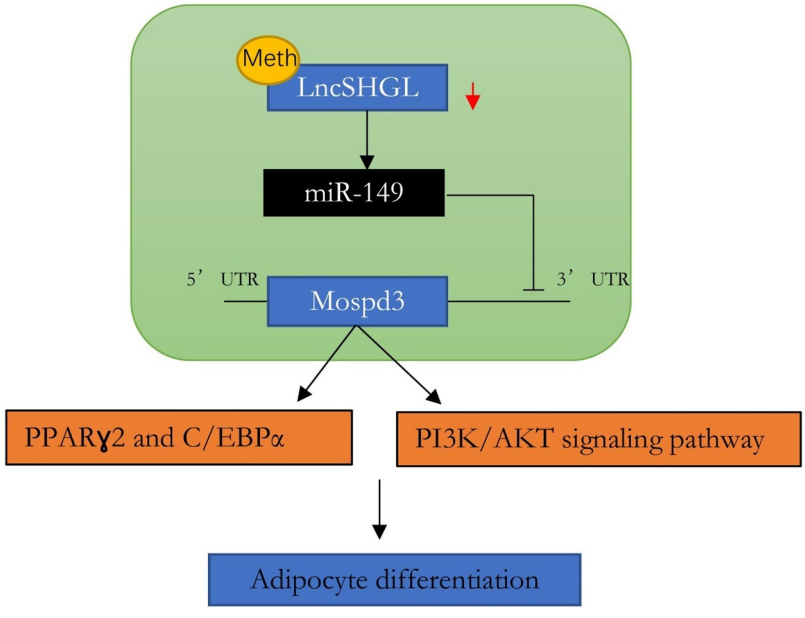

Figure 11. Graphical abstract. Methylation of LncSHGL promotes adipocyte differentiation via regulating miR-149/Mospd3 axis. the expression of lncSHG was downregulated affected by DNA methylation and then the Mospd3 was downregulated by sponging miR-149. Finally, the lncSHGL mediated miR-149/Mospd3 axis will increase the expression of PPARγ2 and C/EBPα and activate PI3K/AKT signaling pathway that promote adipocyte differentiation.

livers of obese mice, and overexpression of lncSHGL suppressed hepatic gluconeogenesis and lipogenesis [16]. Consistent with a previous study on lncSHGL, we demonstrated that lncSHGL was gradually decreased during 3T3-L1 differentiation and was downregulated in the liver and perirenal fat of ob/ob mice. Further analysis indicated that overexpression of lncSHGL impeded 3T3-L1 preadipocytes differentiation and lipid droplet accumulation both *in vitro* and *in vivo*, indicating that lncSHGL reduced 3T3-L1 preadipocytes differentiation. Mechanistically, lncSHGL promoted adipocyte differentiation by regulating the miR-149/Mospd3 axis. These findings provide a new understanding of the role of lncSHGL in modulating adipogenesis during obesity.

With the advanced development of lncRNAs, many studies have demonstrated that lncRNAs perform biological functions as ceRNAs of miRNA-mRNA networks [31]. For example, Li et al. revealed that the expression of lncRNA HCG11 is reduced during adipogenesis, and further analysis showed that HCG11 inhibits cell proliferation and adipogenesis by sponging miR-204-5p and regulates SIRT1 expression [32]. Guo et al. comprehensively investigated and screened crucial lncRNAmiRNAmRNA interaction axes using microarray datasets and revealed that the RP11-552F3.9-miR-130b-5p/miR-23a-5p-LEP interaction axes may be crucial for inducing adipogenic differentiation [31]. Zhang et al. identified RP11-142A22.4 as a significantly upregulated lncRNA in visceral adipose tissue that promoted adipogenesis by sponging miR-587 to modulate Wnt5β expression [33]. Therefore, we first explored the target miRNAs of lncSHGL using bioinformatics analysis. After validation, miR-149 was identified as a target of lncSHGL. Using miR-149 mimics and inhibitors, we further confirmed the influence of miR-149 on the function of lncSHGL during 3T3-L1 cell differentiation. Therefore, we predicted the targets of miR-149 and Mospd3. Unsurprisingly, downregulating expression of Mospd3 amplified the production of triglycerides and lipid droplets. Finally, we confirmed that lncSHGL acts as a sponge for miR-149, and Mospd3 is a target of miR-149. Further analysis indicated that miR-149 could partially reverse the function of lncSHGL, and Mospd3 knockdown reversed the function of miR-149 inhibitor on adipocyte differentiation and lipid droplet accumulation. PPAR-γ and C/EBPα act as two adipocyte master transcription factors that play crucial roles in adipogenesis [34]. Overexpression of LncSHGL downregulated PPARγ2 and C/EBPα expression by regulating promotor of PPARγ2 and C/EBPα *via* regulating miR-149/Mospd3 expression. These results indicated that lncSHGL regulated PPARγ2 and C/EBPα expression by regulating promotor of PPARγ2 and C/EBPα *via* miR-149/Mospd3 axis which could affect the 3T3-L1 preadipocytes differentiation.

The differentiation of precursor adipose stem cells into mature adipocytes is one of the most important reasons for adipose tissue hyperplasia [35]. Differentiation of pre-adipocytes into mature adipocytes is a key process involving the coordinated expression of specific genes [3]. To determine the signaling pathways affected by lncSHGL, the differentially expressed genes between the low and high lncSHGL expression groups were subjected to GO and KEGG enrichment analyses. GO enrichment KEGG analysis illustrated that PI3K-AKT was the most significantly enriched signaling pathway between low and high lncSHGL expression. The PI3K-AKT signaling pathway is one of the most important signaling pathways currently studied for adipocyte differentiation. Cai et al. indicated that lnc-ORA is highly expressed in ob/ob mice, and knockdown of lnc-ORA inhibited adipocyte differentiation by regulating the PI3K/AKT/mTOR signaling pathway [36]. Furthermore, He et al. showed that SNORD126 promoted adipogenesis in cells and rats by activating the PI3K-AKT pathway [37]. In this study, we found that phosphorylated PI3K, AKT, and mTOR were significantly downregulated after lncSHGL overexpression but upregulated when cells were silenced with lncSHGL. Further analysis indicated that the reduction in phosphorylated PI3K, AKT, and mTOR levels caused by lncSHGL overexpression was partially reversed in the presence of miR-149 mimics. In addition, suppression of Mospd3 also increased the expression of phosphorylated PI3K, AKT, and mTOR in 3T3-L1 adipocytes in the presence of the miR-149 inhibitor both *in vitro* and *in vivo*. These results suggest that the lncSHGL/miR-149/Mospd3 axis modulates the

PI3K/AKT/mTOR signaling pathway, which in turn regulates cell proliferation, differentiation, and production of triglycerides and lipid droplets in the cells and livers of obese mice.

DNA methylation is a significant epigenetic regulation of the eukaryotic cell genome and is inseparable from the development of vascular diseases, as well as in adipocyte differentiation [38]. Liu et al. demonstrated that adipocyte differentiation and lipid deposition could be enhanced by ColXV by reducing DNA methylation and repressing the cAMP/PKA signaling pathway [39]. Hoxa5 promotes adipose differentiation by increasing DNA methylation levels and inhibiting the PKA/HSL signaling pathway in mice [40]. Thus, we considered whether methylation of lncSHGL affects the expression of wild type lncSHGL. First, we found that DNA methylation level and the expression of DNMT1 and LPL, PPARγ2, AP2, and C/EBPα were dramatically elevated in MDI stimulated group while was significantly inhibited after cells treated with 5-Aza-dC, which is an inhibitor of DNMT1, suggesting that DNA methylation participated in the 3T3-L1 cell differentiation. In addition, we found that lncSHGL expression was dramatically upregulated upon treatment with 5-Aza-dC, suggesting that lncSHGL expression is affected by DNA methylation. Moreover, we validated the function of lncSHGL in adipogenesis using a mouse model of obesity. We found that low lncSHGL expression was observed in the liver, perirenal fat, and subcutaneous fat of ob/ob mice, but not in control mice. Interestingly, we observed overexpressed lncSHGL in ob/ob mice with overexpressed lncSHGL only in the liver, but not in perirenal fat and subcutaneous fat. Consistent with lncSHGL expression, downregulation of miR-149 and upregulation of Mospd3 were observed in ob/ob mice overexpressing lncSHGL. Overexpression of lncSHGL induced a decrease in the production of triglycerides and cholesterol, which was consistent with the reduced expression of adipogenesis-related genes. Finally, an upregulated signaling pathway of PI3K/AKT/mTOR was observed in the livers of ob/ob mice after lncSHGL overexpression. Taken together, we demonstrated that methylation of lncSHGL may promote adipocyte differentiation by regulating the miR-149/Mospd3 axis involved in the PI3K/AKT signaling pathway *in vitro* and *in vivo*.

Conclusion

Our study revealed that lncSHGL expression declines during the differentiation of 3T3-L1 cells. Through further investigation, we were able to demonstrate that suppression of lncSHGL expression promotes adipocyte differentiation by regulating the miR-149/Mospd3 axis and PI3K/AKT signaling pathway. Additionally, we found that DNA methylation of lncSHGL plays a vital role in this process. These findings suggest that modulating lncSHGL expression may be a promising therapeutic target for adipogenesis in obesity, particularly in cases of fatty liver disease.

Disclosure statement

No potential conflict of interest was reported by the author(s).

Funding

This The present study was supported by Nature Science Foundation of Fujian Province (No: 2020J011234; No: 2020J011227)

Authors' contributions

Conceptualization, X.H. and J.L.; methodology, X.H. and X.L.; software, X.H.; validation, X.H., X.L. and J.L.; formal analysis, M. M., M.P. and W.K.; investigation, X.H., X.L. and J.L; resources, X.H., X.L. and J.L.; data curation, X.H.; writing – original draft preparation, X.H; writing – review and editing, X.H., X.L and J. L; visualization, X.H.; supervision, J.L.; project administration, J. L.; funding acquisition, X.H. and J.L. All authors have read and agreed to the published version of the manuscript.

Availability of data and materials

The datasets used and/or analyzed during the current study are available from the corresponding author on reasonable request.

Consent for publication

We have obtained consent to publish from the participants to report patient data.

Ethics approval and consent to participate

The study was reviewed and approved by the ethics committee of the first Affiliated Hospital of Xiamen University (Xiamen, China).

References

[1] Mayoral LP, Andrade GM, Mayoral EP, et al. Obesity subtypes, related biomarkers & heterogeneity. Indian J Med Res. 2020 Jan;151(1):11–21. doi: 10.4103/ijmr.IJMR_1768_17

[2] Ghaben AL, Scherer PE. Adipogenesis and metabolic health. Nat Rev Mol Cell Biol. 2019 Apr;20(4):242–258. doi: 10.1038/s41580-018-0093-z

[3] Sarantopoulos CN, Banyard DA, Ziegler ME, et al. Elucidating the preadipocyte and its role in adipocyte formation: a comprehensive review. Stem Cell Rev And Rep. 2018 Feb;14(1):27–42. doi: 10.1007/s12015-017-9774-9

[4] Benchamana A, Mori H, MacDougald OA, et al. Regulation of adipocyte differentiation and metabolism by lansoprazole. Life Sci. 2019 Dec 15;239:116897. doi: 10.1016/j.lfs.2019.116897

[5] Raza SHA, Khan R, Cheng G, et al. RNA-Seq reveals the potential molecular mechanisms of bovine KLF6 gene in the regulation of adipogenesis. Int j biol macromol. 2022;195:198–206. doi: 10.1016/j.ijbiomac.2021.11.202

[6] Raza SHA, Khan R, Schreurs NM, et al. Expression of the bovine KLF6 gene polymorphisms and their association with carcass and body measures in Qinchuan cattle (Bos Taurus). Genomics. 2020;112(1):423–431. doi: 10.1016/j.ygeno.2019.03.005

[7] Yang Q, Wan Q, Zhang L, et al. Analysis of LncRNA expression in cell differentiation. RNA Biol. 2018 Mar 4;15(3):413–422. doi: 10.1080/15476286.2018.1441665

[8] Lee JT. Epigenetic regulation by long noncoding RNAs. Science. 2012 Dec 14;338(6113):1435–1439. doi: 10.1126/science.1231776

[9] Zhang W, Sun B, Zhao Y, et al. Proliferation of bovine myoblast by LncPRRX1 via regulation of the miR-137/CDC42 axis. Int j biol macromol. 2022;220:33–42. doi: 10.1016/j.ijbiomac.2022.08.018

[10] Ma X, Yang X, Zhang D, et al. RNA-seq analysis reveals the critical role of the novel lncRNA BIANCR in intramuscular adipogenesis through the ERK1/2 signaling pathway. J Anim Sci Biotechnol. 2023;14(1):21. doi: 10.1186/s40104-022-00820-1

[11] Wang Z, Luo Z, Dai Z, et al. Long non-coding RNA lnc-OAD is required for adipocyte differentiation in 3T3-L1 preadipocytes. Biochem Biophys Res Commun. 2019 Apr 16;511(4):753–758. doi: 10.1016/j.bbrc.2019.02.133

[12] Chen J, Jin J, Zhang X, et al. Microglial lnc-U90926 facilitates neutrophil infiltration in ischemic stroke via MDH2/CXCL2 axis. Mol Ther. 2021;29(9):2873–2885. doi: 10.1016/j.ymthe.2021.04.025

[13] Chen J, Liu Y, Lu S, et al. The role and possible mechanism of lncRNA U90926 in modulating 3T3-L1 preadipocyte differentiation. Int J Obes (Lond). 2017 Feb;41(2):299–308. doi: 10.1038/ijo.2016.189

[14] Chen Z, Luo Y, Yang W, et al. Comparison analysis of dysregulated lncrna profile in mouse plasma and liver after hepatic ischemia/reperfusion injury. PLoS One. 2015;10(7):e0133462. doi: 10.1371/journal.pone.0133462

[15] Chen Z, Jia S, Li D, et al. Silencing of long noncoding RNA AK139328 attenuates ischemia/reperfusion injury in mouse livers. PLoS One. 2013;8(11):e80817. doi: 10.1371/journal.pone.0080817

[16] Wang J, Yang W, Chen Z, et al. Long noncoding RNA lncSHGL recruits hnRNPA1 to suppress hepatic gluconeogenesis and Lipogenesis. Diabetes. 2018 Apr;67(4):581–593. doi: 10.2337/db17-0799

[17] Yang X, Mei C, Raza SHA, et al. Interactive regulation of DNA demethylase gene TET1 and m6A methyltransferase gene METTL3 in myoblast differentiation. Int j biol macromol. 2022;223(Pt A):916–930. doi: 10.1016/j.ijbiomac.2022.11.081

[18] Yang X, Ning Y, Abbas Raza SH, et al. MEF2C expression is regulated by the post-transcriptional activation of the METTL3-m6A-YTHDF1 axis in myoblast differentiation. Front Vet Sci. 2022;9:900924. doi: 10.3389/fvets.2022.900924

[19] Yang J, Yang Q, Huang X, et al. METTL3-mediated LncRNA EN_42575 m6A modification alleviates CPB2 toxin-induced damage in IPEC-J2 cells. Int J Mol Sci. 2023;24(6):5725. doi: 10.3390/ijms24065725

[20] Wang Z, He J, Bach D-H, et al. Induction of m6A methylation in adipocyte exosomal LncRNAs mediates myeloma drug resistance. J Exp Clin Cancer Res. 2022;41(1):4. doi: 10.1186/s13046-021-02209-w

[21] Mueller E. Understanding the variegation of fat: novel regulators of adipocyte differentiation and fat tissue biology. Biochim Biophys Acta. 2014 Mar;1842(3):352–357. doi: 10.1016/j.bbadis.2013.05.031

[22] Andrés-Manzano MJ, Andrés V, Dorado B. Oil Red O and hematoxylin and eosin staining for quantification of atherosclerosis burden in mouse aorta and aortic root. Methods Mol Biol. 2015;1339:85–99.

[23] Schneider CA, Rasband WS, Eliceiri KW. NIH image to ImageJ: 25 years of image analysis. Nat Methods. 2012;9(7):671–675. doi: 10.1038/nmeth.2089

[24] Wang W, Pan Y, Wang L, et al. Optimal dietary ferulic acid for suppressing the obesity-related disorders in leptin-deficient obese C57BL/6J -ob/ob mice. J Agric Food Chem. 2019;67(15):4250–4258. doi: 10.1021/acs.jafc.8b06760

[25] Ndumele CE, Nasir K, Conceiçao RD, et al. Hepatic steatosis, obesity, and the metabolic syndrome are independently and additively associated with increased systemic inflammation. Arterioscler Thromb Vasc Biol. 2011;31(8):1927–1932. doi: 10.1161/ATVBAHA.111.228262

[26] Sommer A, Twig G. The impact of childhood and adolescent obesity on cardiovascular risk in adulthood: a systematic review. Curr Diab Rep. 2018 Aug 30;18(10):91. doi: 10.1007/s11892-018-1062-9

[27] Piche ME, Tchernof A, Despres JP. Obesity phenotypes, diabetes, and cardiovascular diseases. Circ Res. 2020 May 22;126(11):1477–1500. doi: 10.1161/CIRCRESAHA.120.316101

[28] Zhu E, Zhang J, Li Y, et al. Long noncoding RNA Plnc1 controls adipocyte differentiation by regulating peroxisome proliferator-activated receptor gamma. FASEB J. 2019 Feb;33(2):2396–2408. doi: 10.1096/fj.201800739RRR

[29] Zhang L, Zhang D, Qin ZY, et al. The role and possible mechanism of long noncoding RNA PVT1 in modulating 3T3-L1 preadipocyte proliferation and differentiation. IUBMB Life. 2020 Jul;72(7):1460–1467. doi: 10.1002/iub.2269

[30] Yi F, Zhang P, Wang Y, et al. Long non-coding RNA slincRAD functions in methylation regulation during the early stage of mouse adipogenesis. RNA Biol. 2019 Oct;16(10):1401–1413. doi: 10.1080/15476286.2019.1631643

[31] Chen K, Xie S, Jin W. Crucial lncRnas associated with adipocyte differentiation from human adipose-derived stem cells based on co-expression and ceRNA network analyses. PeerJ. 2019;7:e7544. doi: 10.7717/peerj.7544

[32] Li D, Liu Y, Gao W, et al. LncRNA HCG11 inhibits adipocyte differentiation in human adipose-derived mesenchymal stem cells by sponging miR-204-5p to upregulate SIRT1. Cell Transplant. 2020 Jan-Dec ;29:963689720968090.

[33] Zhang T, Liu H, Mao R, et al. The lncRNA RP11-142A22.4 promotes adipogenesis by sponging miR-587 to modulate Wnt5beta expression. Cell Death Dis. 2020 Jun 19;11(6):475. doi: 10.1038/s41419-020-2550-9

[34] Wang G, Wu B, Zhang L, et al. Laquinimod prevents adipogenesis and obesity by down-regulating PPAR-gamma and C/EBPalpha through activating AMPK. ACS Omega. 2020 Sep 15;5(36):22958–22965. doi: 10.1021/acsomega.0c02525

[35] Ong BX, Brunmeir R, Zhang Q, et al. Regulation of thermogenic adipocyte differentiation and adaptive thermogenesis through histone acetylation. Front Endocrinol. 2020;11:95. doi: 10.3389/fendo.2020.00095

[36] Cai R, Tang G, Zhang Q, et al. A novel lnc-RNA, named lnc-ORA, is identified by RNA-Seq analysis, and its knockdown inhibits adipogenesis by regulating the PI3K/AKT/mTOR Signaling pathway. Cells. 2019 May 18;8(5):477. doi: 10.3390/cells8050477

[37] He Y, Wu Y, Mei B, et al. A small nucleolar RNA, SNORD126, promotes adipogenesis in cells and rats by activating the PI3K-AKT pathway. J Cell Physiol. 2021 Apr;236(4):3001–3014. doi: 10.1002/jcp.30066

[38] Vera-Perez B, Arribas MI, Vicente-Salar N, et al. DNA methylation profile of different clones of human adipose stem cells does not allow to predict their differentiation potential. J Histotechnol. 2019 Dec;42(4):183–192. doi: 10.1080/01478885.2019.1655962

[39] Liu G, Li M, Xu Y, et al. ColXV promotes adipocyte differentiation via inhibiting DNA methylation and cAMP/PKA pathway in mice. Oncotarget. 2017 Sep 1;8(36):60135–60148. doi: 10.18632/oncotarget.18550

[40] Cao W, Xu Y, Luo D, et al. Hoxa5 promotes adipose differentiation via Increasing DNA methylation level and inhibiting PKA/HSL signal pathway in mice. Cell Physiol Biochem. 2018;45(3):1023–1033. doi: 10.1159/000487343